Melting of a porous iron particle in slag

BGUM 2025

Jean Robin[1,2], Cesar Pairetti[2], Edouard Izard[1], Aliyeh Rafiei[3], Stéphane Zaleski[2]

[1]Institut Jean Le Rond d'Alembert, Sorbonne Université,
[2]ArcelorMittal Maizières Research
[3]ArcelorMittal Global RD Hamilton

July 7-9, 2025

Direct Reduced Iron

Spherical porous iron particle

- Mean diameter $d_{DRI} \approx 1cm$
- Porosity $\Phi \approx 40 - 70\%$
- Pore size $d_{por} \approx 1 - 20\mu m$
- Mean density $\rho_{DRI} \approx 2000 - 4000 kg.m^{-3}$

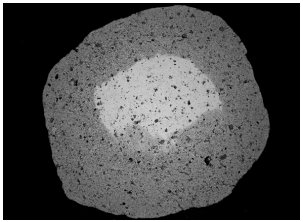

Fig. 1: SEM analysis of a DRI pellet

Industrial furnace

- furnace diameter $\approx 15m$
- DRI forming large banks above slag surface

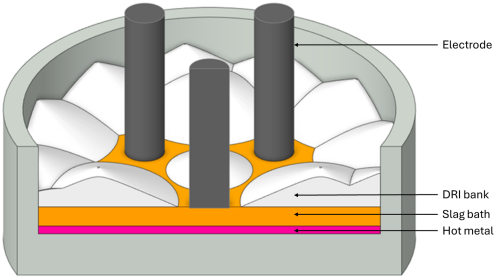

Fig. 2: Schematic representation of an industrial furnace

Experimental Melting Study

- Melting of a single pellet
- Small crucible ($d < 10cm$)
- X-Ray fluoroscopy

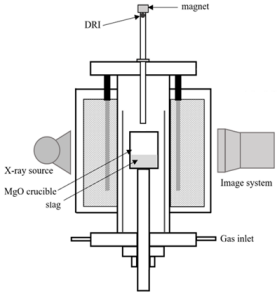

Fig. 3: Experimental set-up[1]

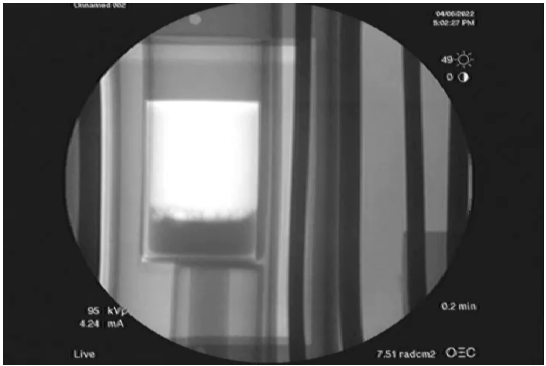

Fig. 4: Melting of H-DRI in slag heated at 1600 °C

[1] A. Rafiei and S. Sun *ArcelorMittal Global RD Hamilton*, *McMaster University*, 2024

Observed particle behavior

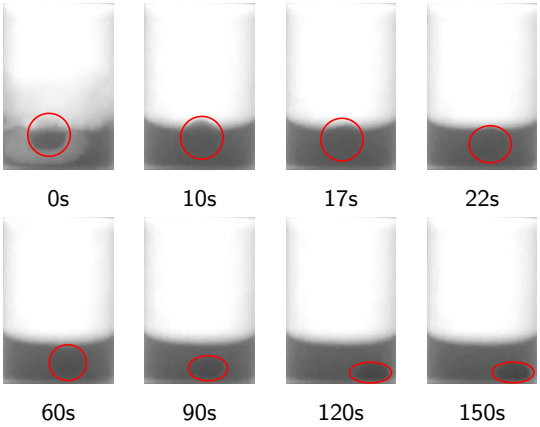

Observations

- Particle starts to sink after $\approx 10s$
- Particle keeps it shape and volume during sinking
- Particle shrinks and looses the spherical shape after $\approx 180s$

Conclusions

- Melting point is reached at 180s
- Particle sinks before melting point is reached
- Particle gain mass as slag infiltrate its pores

Pellet Properties model

Hypothesis

- Uniformly distributed porosity
- Same size for all pores

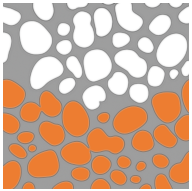

Fig. 5: Representation of the DRI porous structure

- Introduction of tracer inside the pellet

$$\alpha = \begin{cases} 0 & \text{for gas in the pores} \\ 1 & \text{for slag in the pores} \end{cases}$$

- Pore properties

$$\chi_{por} = \alpha\chi_{slag} + (1-\alpha)\chi_{air}$$

- Viscosity

$$\mu_{DRI} = \mu_{met}$$

- Density

$$\rho_{DRI} = \Phi\rho_{por} + (1-\Phi)\rho_{met}$$

- Heat Capacity

$$C_{p_{DRI}} = \Phi C_{p_{por}} + (1-\Phi)C_{p_{met}}$$

- Thermal Conductivity

$$\lambda_{DRI} = c\frac{\lambda_{met}(1-\Phi) + \lambda_{por}\Phi\frac{3\lambda_{met}}{2\lambda_{met}+\lambda_{por}}}{(1-\Phi) + \Phi\frac{3\lambda_{met}}{2\lambda_{met}+\lambda_{por}}}$$

Slag Penetration - Darcy Model

- Spherical particle fully immersed in hot slag
- Isentropic configuration for 1D domain src/spherisym.h

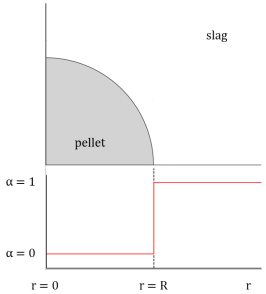

Fig. 6: Initial tracer field - fully immersed pellet

Darcy - Fourier model

- Darcy Flow model

$$\begin{aligned} \langle \mathbf{u} \rangle &= \frac{K}{\mu_f}(\langle \rho_f \rangle \mathbf{g} - \nabla \langle P_f \rangle + \nabla \pi_c) \\ K &= \frac{d^2 \Phi^3}{180(1-\Phi)^2} \\ \Delta \pi_c &= \frac{2\gamma \cos(\theta)}{r} \end{aligned}$$

- Tracer advection

$$\partial_t \alpha + \langle \mathbf{u} \rangle \cdot \nabla \alpha = 0$$

- Energy equation

$$\partial_t \langle T \rangle + \langle \mathbf{u} \rangle \cdot \nabla \langle T \rangle = \nabla \cdot (\kappa \nabla \langle T \rangle)$$

Temperature-dependent Properties

- Thermal properties

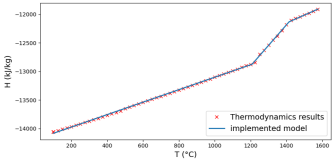

Fig. 7: Slag enthalpy of an EAF slag

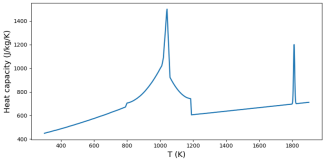

Fig. 8: Heat capacity of Iron

- Rheological property

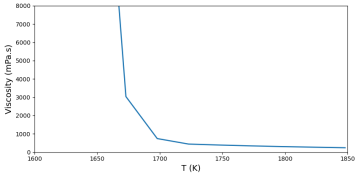

Fig. 9: Slag viscosity

Slag Penetration Results - Darcy Model

- Cold pellet fully immersed in cold slag
- Pores initially filled with air

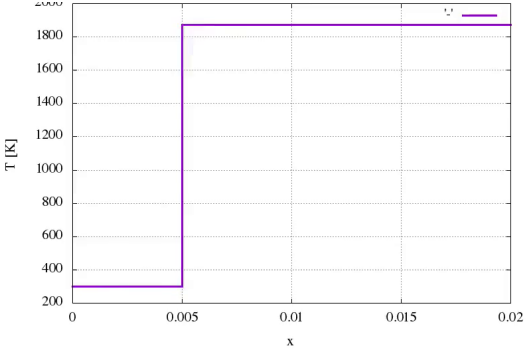

Fig. 10: Temperature profil along pellet radius

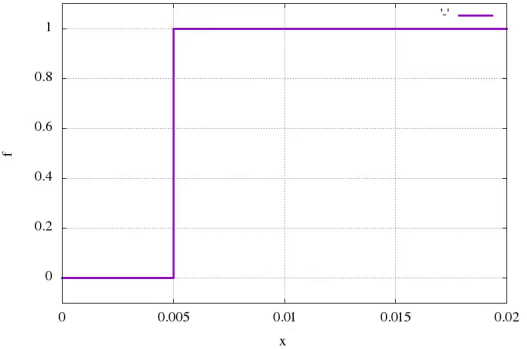

Fig. 11: Slag fraction in the pores along pellet radius

Slag Penetration - Physical Phenomena

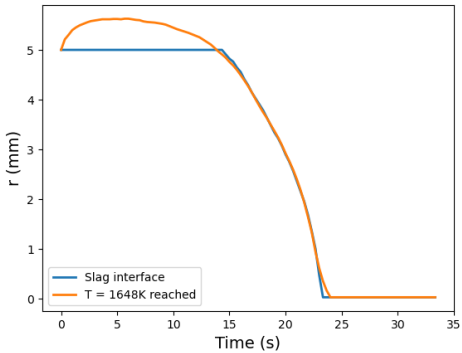

Fig. 12: Evolution of Slag interface and melting point along pellet radius over time

The heating and melting of the pellet is decomposed in 3 phases.

- Solid shell around the pellet prevents any slag flow inside the pellet. The heat transfer is caused by conduction.
- The solid shell has melted, and the slag can flow through the pore entire network.
- The slag fills completely the pore network and stops flowing. The heat transfer is a result of conduction.

Slag Penetration - Temperature Dependent Model

- Temperature diffusion limiting slag penetration
- Pore composition can be determined based on temperature

$$\alpha = \begin{cases} 0 & \text{if } T < T_{liq}, \\ 1 & \text{otherwise,} \end{cases}$$

- Energy equation can determine pore properties and composition

$$\partial_t \langle T \rangle = \nabla \cdot (\kappa \nabla \langle T \rangle)$$

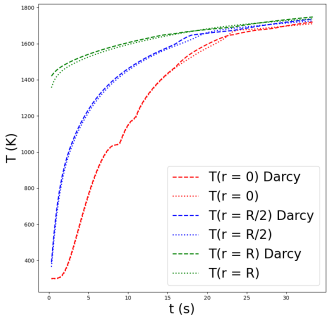

Fig. 13: Temperature profiles evolution for Darcy case and pure diffusive case

Temperature transport model validation

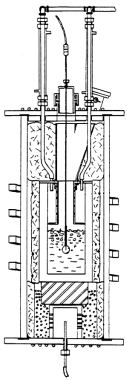

Fig. 14: Experimental set-up[2]

- Melting of a single pellet
- Fully immersed pellet in EAF slag at 1400 °C
- Isentropic configuration

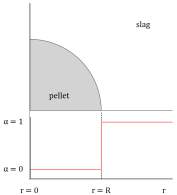

Fig. 15: Initial tracer field - fully immersed pellet

- Temperature diffusion

$$\partial_t \langle T \rangle = \nabla \cdot (\kappa \nabla \langle T \rangle)$$

- Pore composition

$$\alpha = \begin{cases} 0 & \text{if } T < T_{liq}, \\ 1 & \text{otherwise,} \end{cases}$$

- Thermal properties

$$\chi = \chi(\alpha, \Phi, T)$$

[2] R. J. O'Malley, "The heating and melting of metallic DRI particles in steelmaking slags," *Massachusetts Institute of Technology*, 1983

Temperature transport model validation

- Immersed Solid Iron Sphere

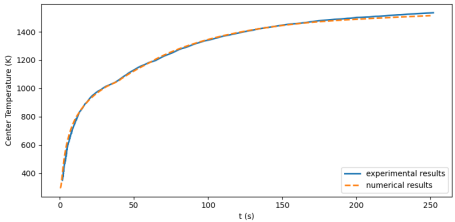

- Lab-Reduced pellets

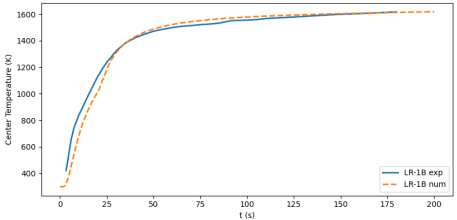

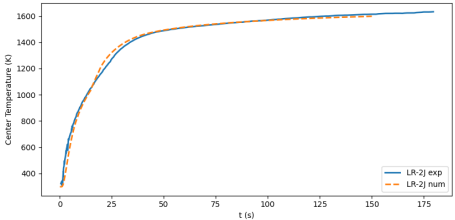

Slag penetration validation?

- Low initial slag temperature $T_i = 1400°C$ ($T_{liq} = 1375°C$)
- Small influence of slag penetration for $T_i = 1600°C$

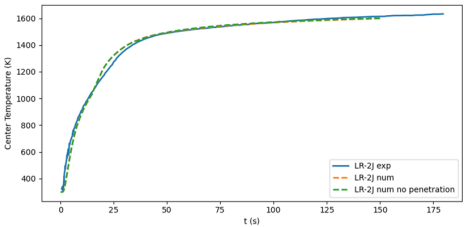

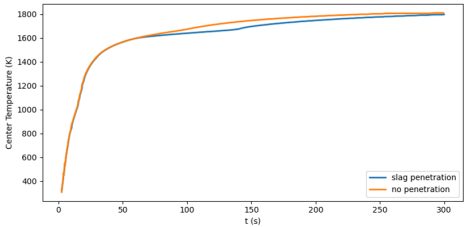

Numerical Simulation of Three-Phase Flow in a crucible

Basilisk flow solver

- One-fluid method for multiphase incompressible Navier-Stokes Equations

$$\frac{\partial \mathbf{u}}{\partial t} + \mathbf{u} \cdot \nabla \mathbf{u} = \frac{1}{\rho}\left[-\nabla p + \nabla \cdot \left(\mu[\nabla \mathbf{u} + \nabla \mathbf{u}^T]\right) + \sigma \kappa \delta \mathbf{n}\right] + \mathbf{g}$$

$$\nabla \cdot \mathbf{u} = 0$$

- Interface advected with split geometric VOF: Three phases tracked explicitly

$$\frac{\partial f_n}{\partial t} + \mathbf{u} \cdot \nabla f_n = 0$$

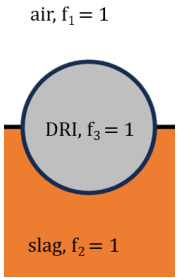

- Three-phase CSF surface tension formulation [3]
- Temperature Transport Equation

$$\partial_t T + \mathbf{u} \cdot \nabla T = \nabla \cdot (\kappa \nabla T)$$

[3] C. Zhao, J. Maarek, S. M. Taleghani, and S. Zaleski, "A hybrid continuum surface tension force for the three-phase vof method," *Journal of Computational Physics*, vol. 504, p. 112872, 2024

Pellet dropped in a crucible

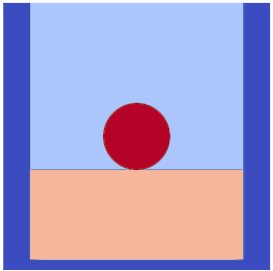

Fig. 16: Melting Pellet

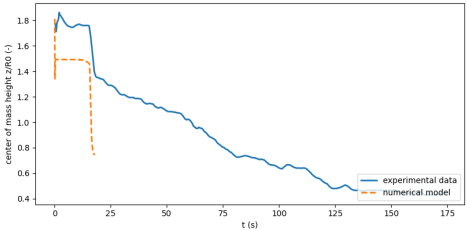

Fig. 17: Pellet center of mass evolution comparison between experimental data and simulation results for a DRI pellet immersed in an EAF slag at 1600 °C

Conclusion

- A model describing the slag invasion of a melting DRI particle was developed.
- Hypothesis made on pore composition depending only on temperature.
- Good agreement with experimental data for temperature transport.
- Good agreement with experimental data for beginning of slag invasion.

Next Steps

Better description of slag invasion phenomena.

- Adding Forchheimer term in Darcy equation
- Using LTNE instead of LTE
- Using coupled Darcy equations for gas and slag flux
- Exploiting quenching experimental results

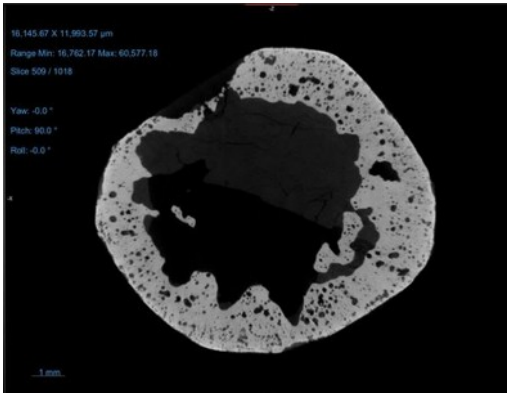

Fig. 18: SEM analysis of a C-DRI melted in a slag at 1500 °C

Next Steps

Multiple particles melting simulations.

- using no-coalescence.h
- adding tension coefficient between particles
- modeling sintering

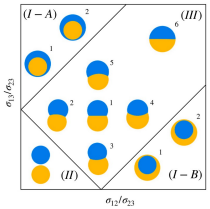

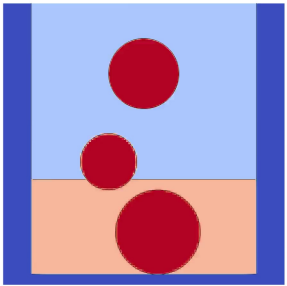

Fig. 19: Morphology diagram of equilibrium shapes[4]

[4] C. Zhao, J. Maarek, S. M. Taleghani, and S. Zaleski, "A hybrid continuum surface tension force for the three-phase vof method," *Journal of Computational Physics*, vol. 504, p. 112872, 2024